Sensors and Materials, Vol. 34, No. 11 (2022) 3923–3931
MYU Tokyo

S & M 3086

Intensity-modulated Refractive Index Sensor Using Tilted Fiber Bragg Grating with Bi_2Te_3 Film as Sensing Material

Feng Lu,[1*] Junsheng Zhang,[2,3] and Yongqiang Zhao[1]

[1]Taiyuan Institute of Technology, Department of Electronic Engineering,
No. 31 Xinlan Road, Taiyuan 030000, China
[2]North University of China, School of Information and Communication Engineering,
No. 3 Xueyuan Road, Taiyuan 030051, China
[3]North University of China, Shanxi Key Laboratory of Signal Capturing & Processing,
No. 3 Xueyuan Road, Taiyuan 030051, China

(Received July 13, 2022; accepted September 12, 2022)

Keywords: bismuth telluride (Bi_2Te_3), tilted fiber Bragg grating (TFBG), refractive index (RI), sensor, intensity

Refractive index (RI) sensors are of importance in many applications since many physical, biochemical, and environmental parameters can be detected by examining RI variations. In this paper, we describe an intensity-modulated RI sensor using a bismuth telluride (Bi_2Te_3)–integrated tilted fiber Bragg grating (TFBG) configuration. Bi_2Te_3 is deposited on the fiber cylindrical surface using magnetron sputtering technology. The light–matter interaction of Bi_2Te_3 is activated, and the optical tunable feature is used for RI measurement. The maximum RI sensitivity is ~333.4 dB/RIU. Furthermore, when the intensity difference between the cladding mode and the core mode is used for RI measurement, the result is immune to light intensity fluctuation. Moreover, the area occupied by all cladding modes is used in the RI sensitivity calculation, thus a wide RI range measurement is realized. To the best of our knowledge, this is the first time that Bi_2Te_3 is used for an optical fiber sensor, and we hope that the idea presented can be found interesting by the sensing community.

1. Introduction

Various refractive index (RI) sensors have been studied for different applications. The main reason is that many physical, biochemical, and environmental parameters can be detected by examining RI variations.[1,2] Over the past decades, the optical fiber sensor has been booming owing to its well-known advantages, namely, compact size, chemical robustness, immunity to electromagnetic interference, and real-time sensing.[3] Many optical fiber RI sensors have been employing technologies such as the tilted fiber Bragg grating (TFBG),[4] long-period grating (LPG),[5] microfiber interferometer,[6] photonic crystal fiber (PCF),[7] and surface plasmon resonance (SPR)[8] have been demonstrated. The TFBG sensors are always based on the wavelength shifts of different cut-off modes, which result in large errors.[9] A hybrid fiber

*Corresponding author: e-mail: lufeng@tit.edu.cn
https://doi.org/10.18494/SAM4006

ISSN 0914-4935

grating cavity using TFBG to form an all-fiber interferometer has been proposed.[10] With this special and interesting configuration, the intensity modulation technique based on total reflected power monitoring is realized. A self-functionalized and high-sensitivity LPG has also been proposed for RI measurement.[11] The sensor consists of a D-shaped optical fiber fabricated by wet chemical etching and an LPFG fabricated by a UV laser periodically writing the polystyrene onto the flat surface of the fiber. Its sensitivity is around 700 nm/RIU for RI = 1.33. Unfortunately, the LPG suffers from the cross-sensitivity of RI and temperature, and the temperature fluctuation leads to a large measurement error.[12] For RI sensors based on PCF and SPR, high cost and a complex manufacturing process are always required.[8] In addition, most of these sensors are based on wavelength modulation instead of intensity modulation, where complex and expensive demodulation devices are required.[13]

In recent years, two-dimensional (2D) layered materials, which include graphene, molybdenum disulfide, and black phosphorus (BP), have attracted significant attention.[14,15] Owing to the exceptional properties of a large surface-to-volume ratio, atomic-thin-layer structure, and high carrier mobility, 2D materials show superior performance in optical modulation for realistic applications in ultrafast lasers, gas detection, and biosensing.[16,17] With the development of Lab-on-Fiber technology, these materials are combined with optical fibers and applied to high-performance sensing of a variety of parameters.[18,19] For example, BP has been introduced as a material for an intensity-modulated optical fiber RI sensor.[20] The BP film is deposited onto the fiber surface by an *in situ* layer-by-layer deposition technique. However, film deposition of 2D materials is challenging owing to the cylindrical geometry and thin diameter of the optical fiber. Apart from 2D materials, topological insulators (TIs) are another type of promising optoelectronic material.[21] The TIs are materials with gapped insulating bulks and metallic conducting surfaces. The strong spin-orbit coupling in TIs lowers the surface resistivity and leads to the formation of a topologically protected surface state. The surface state in TIs has a Dirac electronic spectrum like that of graphene and shows optical properties similar to those of 2D materials. The recently discovered three-dimensional (3D) TIs such as bismuth telluride (Bi_2Te_3) and bismuth selenide (Bi_2Se_3) are referred to as second-generation TIs. These 3D TIs are composed of layered structures in which the adjacent layers are bonded together by weak van der Waals forces.[22] The surface conduction of the material can be further enhanced by making 3D TIs into nanostructures, since the large surface-to-volume ratios of nanoscaled materials maximize the surface contribution to the total conduction.

In this work, we report an integrated Bi_2Te_3–TFBG configuration as an optical tunable platform for RI measurement. The Bi_2Te_3 film is deposited on TFBG by magnetron sputtering. As a result of the interaction between the Bi_2Te_3 film and the cladding mode of TFBG, unique optical tunable properties are observed. The Bi_2Te_3–TFBG sensor exhibits the ability of RI measurement by intensity demodulation.

2. Materials and Methods

2.1 Bi_2Te_3 deposition on TFBG

The TFBG is inscribed in a photosensitive fiber (Fibercore PS750) by the phase-mask technique. The schematic illustration of the TFBG is shown in Fig. 1(a), where Λ is the normal period of the grating and θ denotes the tilt angle of the grating planes relative to the plane of the fiber cross section. The core mode resonance wavelength λ_{Bragg} and the ith cladding mode wavelength $\lambda_{i,\ clad}$ are governed by phase-matching theory, which gives the wavelength position of the resonance band corresponding to the coupling between two modes.[23]

The schematic of the TFBG with a thin Bi_2Te_3 film is shown in Fig. 1(b). Magnetron sputtering is used for Bi_2Te_3 film deposition. Before deposition, the optical fiber over the TFBG region is rinsed with pure acetone to clean the surface of any contaminants. Then, the optical fiber is immersed in deionized water and washed thoroughly. Thereafter, the Bi_2Te_3 film is deposited on the optical fiber by the magnetron sputtering system. During the deposition process, both sides of the optical fiber are held by the holder, as shown in Fig.2. The optical fiber rotates around its axis while rotating around the center of the magnetron sputtering system to obtain a uniform deposition effect. The working pressure is 7.5 mTorr in a pure argon atmosphere. The radio frequency power is set to 60 W. The Bi_2Te_3 target is 2 inches in diameter and 99.999% pure (ZhongNuo Advanced Material). The thickness of the Bi_2Te_3 film is calculated from the deposition rate and experimentally determined under the same conditions.

2.2 Experimental setup

The experimental setup is shown in Fig. 3. A broadband source (BBS) with a wavelength range of 1520 to 1570 nm is utilized as input light. The light passes down the integrated Bi_2Te_3–TFBG sensor through the three-ring polarization controller (PC). The PC is used to adjust the

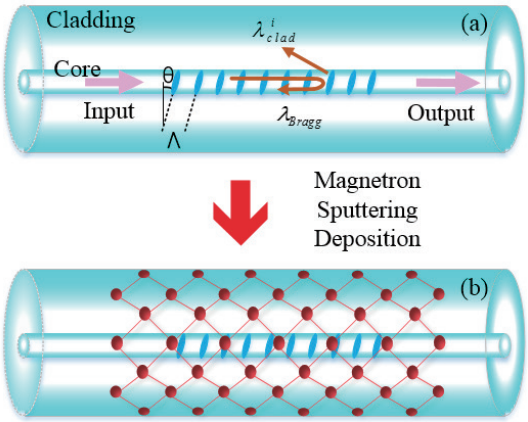

Fig. 1. (Color online) Schematic of Bi_2Te_3–TFBG configuration as an optical tunable platform for strong light–matter interaction. (a) Schematic of TFBG. (b) Schematic of Bi_2Te_3–TFBG configuration.

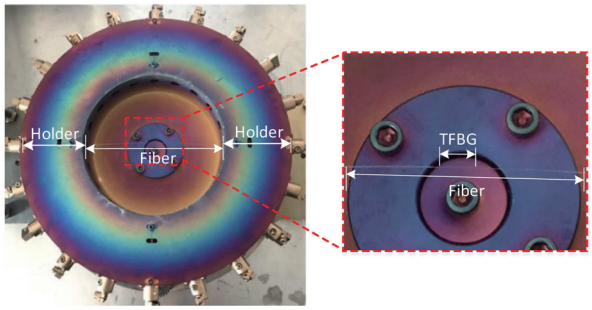

Fig. 2. (Color online) Photograph of optical fiber fixed in magnetron sputtering system.

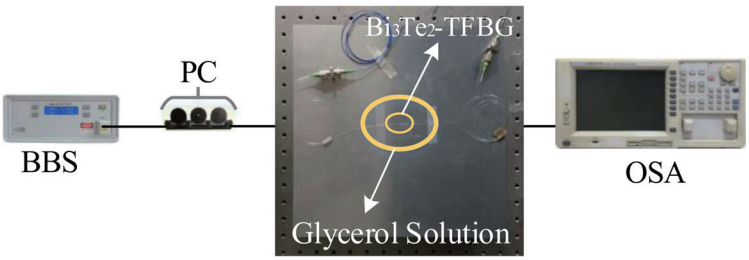

Fig. 3. (Color online) Experimental setup for RI measurement using the Bi_2Te_3–TFBG sensor.

polarization state of the input light. The three rings of the PC are a 1/4-wave plate, half-wave plate and 1/4 wave plate. By adjusting the positions of the three rings, the polarization state of the input light is kept stable. In this way, the measurement error caused by the change of polarization state can be eliminated. The optical fiber with Bi_2Te_3–TFBG is pasted onto the stainless-steel plate. The Bi_2Te_3–TFBG is immersed in glycerol solution. Different RI can be provided by using different concentrations of the glycerol solution. The output spectrum of the Bi_2Te_3–TFBG is detected with an optical spectrum analyzer (OSA: AQ6317B, YOKOGAWA) with a wavelength resolution of 0.02 nm. The experiment is carried out at a constant room temperature of 24.5 °C. Since the amplitude of the TFBG cladding mode is not affected by temperature,[9] the measurement results caused by temperature fluctuations can be ignored.

Here, the overlapped transmission spectra of the TFBG before and after Bi_2Te_3 deposition are shown in Fig. 4. The thickness of the Bi_2Te_3 film is 60 nm. As can be seen from the figure, the cladding mode shows a clear intensity decrease after the Bi_2Te_3 deposition. This phenomenon is attributed to the intense light absorption of Bi_2Te_3, which reduces the coupling efficiency of the light from the fiber core to the cladding. Four cladding modes (marked as "C1", "C2", "C3", and "C4") and the core mode (marked as "B1") are chosen for intensity monitoring in the following experiments.

3. Experimental Results and Discussion

The RI response of a bare TFBG without the Bi_2Te_3 film is studied first. The experiments are conducted with the setup shown in Fig. 2. The transmission spectra of the bare TFBG at different RIs are shown in Fig. 5. It can be seen that, as the RI increases, more and more cladding modes

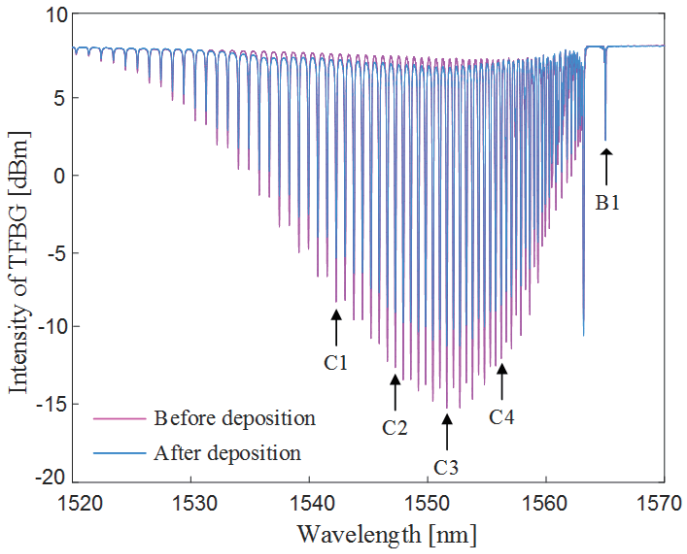

Fig. 4. (Color online) Transmission spectrum of TFBG before and after Bi_2Te_3 deposition.

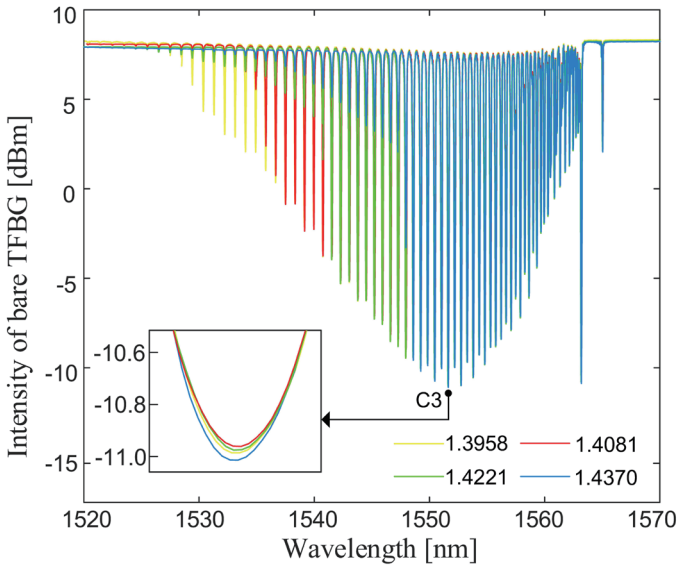

Fig. 5. (Color online) Transmission spectrum of bare TFBG versus RI.

in the short-wavelength direction no longer exist. On the other hand, the intensity of the existing cladding modes is almost stable, as shown in the inset. The result is consistent with the RI response of TFBG reported previously.[4]

The RI response of Bi_2Te_3–TFBG with the film thickness of 60 nm is studied. Figure 6 presents the evolution of the transmission spectra with respect to RI. The spectra measured at different RIs are drawn on the same graph with an offset. It is clear that the RI response in Fig. 6 is completely different from that in Fig. 5. The intensity of the cladding mode changes as the surrounding RI increases, but no cladding mode disappears. Moreover, different cladding modes show different intensity tendencies with the change of the surrounding RI.

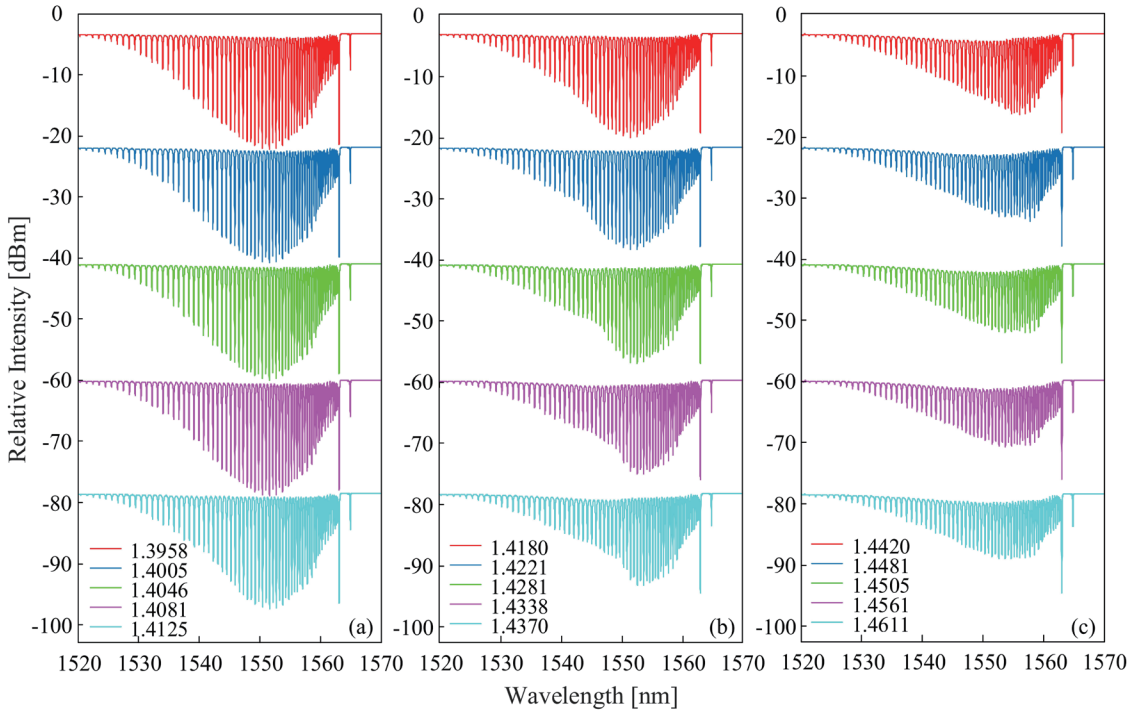

Fig. 6. (Color online) Transmission spectra of Bi_2Te_3–TFBG versus RI: (a) 1.3958–1.4125, (b) 1.4180–1.4370, and (c) 1.4420–1.4611.

Five repeated measurements are conducted under the same experimental conditions. The intensity tendencies of the cladding modes C1, C2, C3, and C4 are illustrated in Figs. 7(a)–7(d), respectively. The standard deviation characterizing the stability of the sensor characteristics is indicated by error bars in the figure. It can be seen that the intensity of the cladding modes decreases gradually in a specific RI range. The cladding mode C3 in Fig. 7(c) shows the maximum sensitivity of ~333.4 dBm/RIU with RI increasing from ~1.43 to ~1.45. The reason for the intensity decrease comes from two aspects. The first one is Bi_2Te_3's exceptional properties of large surface-to-volume ratio and high carrier mobility. Secondly, the carrier concentration of Bi_2Te_3 is changed since the detected solution molecules are absorbed onto the surface of Bi_2Te_3. In this way, the local RI of Bi_2Te_3 is affected. The result is consistent with that of TFBG coated with graphene.[24] However, as clearly shown in Figs. 7(a)–7(d), each cladding mode is only sensitive to a certain RI range. The authors did not determine the causes of this phenomenon. A link to the phase-matching condition of each cladding mode was assumed but not confirmed. On the basis of this special characteristic, a specific cladding mode can be selected for RI measurement in accordance with the RI range to be measured.

Figure 7(e) shows the intensity change of core mode B1, which is almost stable in the same RI range. This means that the intensity of B1 is insensitive to the surrounding RI. In this way, when the intensity difference between the cladding mode and the core mode is used for RI measurement, the result is immune to intensity fluctuation. This is important because intensity fluctuation always leads to a large measurement error in the intensity-modulated measurement system.

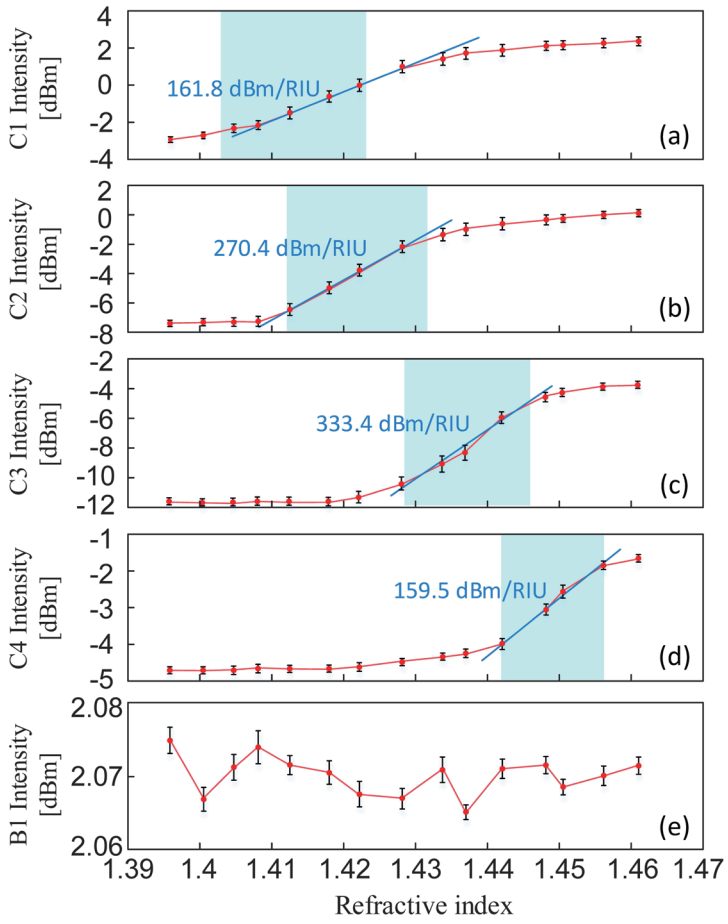

Fig. 7. (Color online) Intensity tendencies of cladding modes (a) C1, (b) C2, (c) C3, (d) C4, and (e) core mode B1.

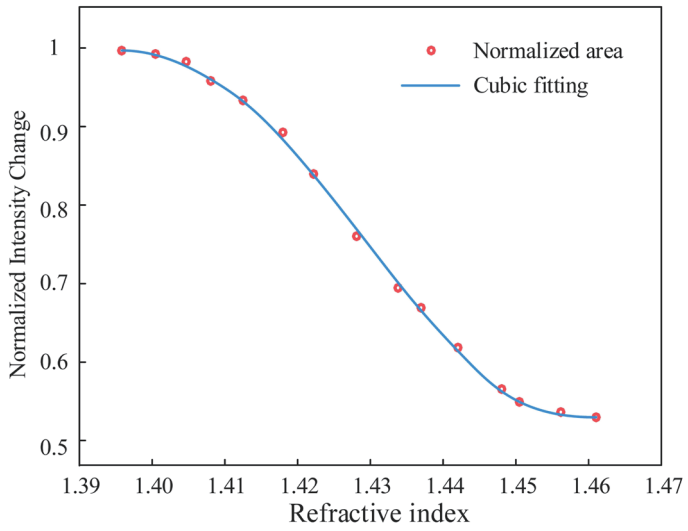

Fig. 8. (Color online) Normalized area changes of all cladding modes.

In addition to using the cladding modes C1, C2, C3, and C4, the area occupied by all cladding modes is also used in the RI sensitivity calculation. Figure 8 shows the total area changes—normalized to the total area of cladding modes of the sensor in air—for the RI range from 1.3958 to 1.4611. The area occupied by all cladding modes decreases as RI increases. The green line presents the cubic nonlinear fitting of the normalized area versus RI. For applications where a wide measurement range is required, the area changes of all cladding modes can be used.

4. Conclusions

We described an integrated Bi_2Te_3–TFBG configuration for RI sensing based on the light–matter interaction of Bi_2Te_3. The light coupling of TFBG can be modulated with Bi_2Te_3 deposition. The maximum RI sensitivity of ~333.4 dBm/RIU is demonstrated in glycerin solution. The proposed configuration proves that the light–matter interaction of Bi_2Te_3 can be used for RI sensing, providing a promising platform for chemical and biochemical applications. Compared with 2D layered materials such as BP, the deposition and thickness of the Bi_2Te_3 film are easier to control, which is more conducive to the consistency and commercialization of the sensor.

Acknowledgments

This work was supported by Key Research and Development Projects of Shanxi Province, (grant number 201803D121069), Scientific and Technological Innovation Programs of Higher Education Institutions in Shanxi Province (grant numbers 2019L0932 and 2020L0624), and the Ministry of Education's Industry University Collaborative Education Program (grant number 202102443002).

References

1 R. Gao, Y. Wang, and X. Xin: Opt. Express **29** (2021) 3. https://doi.org/10.1364/OE.426705
2 X. Liu, C. Shi, J. Hu, H. Wang, H. Han, and J. Zhao: Opt. Commun. **515** (2022) 128171. https://doi.org/10.1016/j.optcom.2022.128171
3 S. Hou, Y. Qin, J. Gao, F. Lyu, and X. Li: Sens. Mater. **33** (2021) 4. https://doi.org/10.18494/SAM.2021.2974
4 Y. Sun, Z. Yan, K. Zhou: J. Lightwave Technol. **39** (2021) 11. https://doi.org/10.1109/JLT.2020.3048981
5 Y. Tan, W. Ji, V. Mamidala, K. Chow, and S. Tjin: Sens. Actuators, B **196** (2014) 9. https://doi.org/10.1016/j.snb.2014.01.063
6 C. R. Liao, T. Y. Hu, and D. N. Wang: Opt. Express **20** (2012) 22813. https://doi.org/10.1364/OE.20.022813
7 Y. Wang, X. Tan, W. Jin, D. Ying, Y.-L. Hoo, and S. Liu: Opt. Lett. **35** (2010) 5. https://doi.org/10.1364/OL.35.000088
8 Y. C. Lin: Sens. Mater. **32** (2020) 12. https://doi.org/10.18494/SAM.2020.2712
9 D. Barrera, J. Madrigal, and S. Sales: Opt. Lett. **42** (2017) 1460. https://doi.org/10.1364/OL.42.001460
10 D. Paladino, G. Quero, C. Caucheteur, P. Mégret, and A. Cusano: Opt. Express **18** (2010) 10473. https://doi.org/10.1364/OE.18.010473
11 G. Quero, A. Crescitelli, D. Paladino, M. Consales, A. Buosciolo, and M. Giordano: Sens. Actuators, B **152** (2011) 196. https://doi.org/10.1016/j.snb.2010.12.007
12 G. Yin, S. Lou, and H. Zou: Opt. Laser Technol. **45** (2013) 4. https://doi.org/10.1016/j.optlastec.2012.06.032
13 Y. Wang, J. Chen, X. Li, X. Zhang, J. Hong, and A. Ye: Opt. Lett. **30** (2005) 8. https://doi.org/10.1364/OL.30.000979
14 J. Miao and C. Wang: Nano Res. **14** (2021) 3. https://doi.org/10.1088/1674-4926/37/9/091001
15 Z. Sun, A. Martinez, and F. Wang: Nat.Photon. **10** (2016) 3. https://doi.org/10.1038/nphoton.2016.15
16 T. Allsop, R. Arif, R. Neal, K.Kalli, and D. J. Webb: Light Sci. Appl. **5** (2016) 12. https://doi.org/10.1038/lsa.2016.36

17 Y. Q. Wang, C. Y. Shen, Wei, and Shen: Appl. Phys. Lett. **109** (2016) 14. https://doi.org/10.1063/1.4959092
18 P. Vaiano, B. Carotenuto, M. Pisco, A. Ricciardi, G. Quero, M. Consales, A. Crescitelli, Esposito, A. Cusano: Laser Photonics Rev. **10** (2016) 6. https://doi.org/10.1002/lpor.201600111
19 Q. Wang and L. Wang: Nanoscale **12** (2020) 7485. https://doi.org/10.1039/D0NR00040J
20 C. Liu, Z. Sun, L. Zhang, J. Lv, X. F. Yu, and X. Chen: Sens. Actuators, B **257** (2018) 22. https://doi.org/10.1016/J.SNB.2017.11.022
21 S. Chen, C. Zhao, Y. Li, H. Huang, S. Lu, and H. Zhang: Opt. Mater. Express **4** (2014) 20. https://doi.org/10.1364/OME.4.000587
22 B. Liu, W. Xie, H. Li, Y. Wang, D. Cai, and D. Wang: Sci. Rep. **4** (2014) 16. https://doi.org/10.1038/SREP04639
23 K. A. Tomyshev, E. I. Dolzhenko, and O. V. Butov: IEEE J. Quantum Electron. **51** (2021) 12. https://doi.org/10.1070/QEL17663
24 B. Jiang, X. Lu, X. Gan, M. Qi, and J. Zhao: Opt. Lett. **40** (2015) 1. https://doi.org/10.1364/OL.40.003994

About the Authors

Feng Lu received his B.S. degree from Shanxi University, Shanxi, China, in 2006 and M. S. degree from Taiyuan University of Technology, Shanxi, China, in 2009. He is currently an associate professor at Taiyuan Institute of Technology. His research interests include optical fiber sensors. (lufeng@tit.edu.cn)

Junsheng Zhang received his B.S. degree from Taiyuan University of Technology, Shanxi, China, in 2003, and M.S. and Ph.D. degrees from North University of China, Shanxi, China, in 2012 and 2020, respectively. His research interests include signal acquisition and intelligent processing. (zhangjs@tit.edu.cn)

Yongqiang Zhao received his B.S. and M.S. degrees from Taiyuan University of Technology, Shanxi, China, in 1991 and 2007, respectively. He is currently a professor and director of the scientific research department at Taiyuan Institute of Technology. His research interests focus on signal and information processing. (zhao-yq2002@163.com)